Analytic parametrization of ^{4}He charge form factor

K. N. Agrawalla and M. K. Parida
Post-Graduate Department of Physics, Sambalpur University, Jyoti Vihar, Burla, Sambalpur 768 017, India
(Received 9 January 1985; revised manuscript received 20 May 1985)

An N/D method of analytic representation for form factors, recently found successful for the deuteron, is used to analyze all the available data on the ^{4}He charge form factor and obtain useful information. The nearest anomalous cut positions in the t plane relevant for this analysis are calculated using possible exchanges at the photon-helium vertex. In contrast to the deuteron case, all familiar and simple intermediate states yield anomalous cut positions above the three-pion cut. Although including the contributions of the three-pion cut in the D function and the five-pion cut in the N function yields a reasonable fit except around the second maximum, the best fit is obtained using the anomalous cut at $t_a=0.247$ GeV^2 instead of the five-pion cut. An exponential weight function, necessary for optimized polynomial expansion in Laguerre polynomials in the N function, seems to be essential in reducing the χ^2 value as in the case of the deuteron. The dip in the form-factor data is parametrized in terms of a zero of the N function and the formula predicts a second zero and a third maximum which can be verified in future experiments. The existing data favor an asymptotic behavior of the type $\exp[-\text{const}(\ln t)^2](\ln t)^4/t^2$ and the formula extrapolates smoothly into the timelike region. A plot of charge density against nuclear radius shows a central depression and the root-mean-square and half-density radii of the distribution are computed.

I. INTRODUCTION

The basic principle of analyticity has been demonstrated to play a very important role in representing the form factors of hadrons and thus, yielding useful information obtainable from data analysis.[1] With a view to testing the applicability of such analytic formulas in the simplest case of nuclear physics, the elastic form factors of deuteron have been successfully parametrized and information has been obtained on the radii of charge and magnetic moment distributions of deuteron, the asymptotic behavior of its form factors, and the magnitudes of the form factors in the timelike region, on extrapolation.[2] But ^{4}He is the lightest isoscalar nucleus for which a large number of unambiguous measurements have been reported on its charge form factors, although in the case of the deuteron such unambiguous results exist only on the magnetic form factors.[2] Further, there is a possibility that the diffractionlike dips observed in the electron-^{4}He elastic scattering cross sections, which appear as structures in the ^{4}He charge form factors, could be parametrized in terms of zeros of an analytic function satisfying the correct analyticity properly in the t plane. Thus, the ^{4}He charge-form-factor data provide an interesting testing ground of the method of analytic representation for light nuclei.[2] In Sec. II of this paper we briefly summarize the method of analytic representation of form factors which takes into account the contributions due to the nearest cuts, including those of the anomalous ones. In Sec. III we compute the positions of the anomalous cuts of the ^{4}He form factor using different exchanges at the electromagnetic vertex. In Sec. IV we examine how far the analytic representation succeeds in describing the charge-form-factor data of ^{4}He. In Sec. V, we report some information relating to the ^{4}He nucleus and its form factor which we obtain from the present analysis. Our conclusions are briefly summarized in Sec. VI.

II. A MODIFIED N/D METHOD OF ANALYTIC REPRESENTATION

The form factor $F(t)$ of a hadron or a light nucleus is proposed to satisfy the representation[1,2]

$$F(t)=N(t)/D(t)\ , \tag{1}$$

where the $D(t)$ function is taken to represent the contribution of the nearest physical cut and the $N(t)$ function that of the other cut which can be parametrized by conformal mapping and optimized polynomial expansion[3,4] (OPE). For isoscalar target nuclei, the nearest three-pion-cut contribution can be parametrized as[2]

$$D(t)=\sum_n a_n t^n+h(t)+\frac{2}{3}\frac{m_\pi{}^2}{\pi}\ , \tag{2}$$

where

$$h(t)=\frac{2}{\pi}\frac{k^3}{\sqrt{t}}\ln\left[\left[\frac{t}{9m_\pi{}^2}\right]^{1/2}+\left[\frac{t}{9m_\pi{}^2}-1\right]^{1/2}\right]-i\frac{k^3}{\sqrt{t}} \tag{3}$$

with

$$k=(t/9-m_\pi{}^2)^{1/2}\ .$$

The fact that the $D(t)$ function contains the threshold structure corresponding to the nearest three-pion cut can be verified from the twice-subtracted dispersion relation,

$$h(t)=\frac{1}{\pi}\left[-\frac{2}{3}m_\pi^2+\frac{8t}{81}-t^2\int_{9m_\pi^2}^{\infty}\frac{(t/9-m_\pi^2)^{3/2}dt'}{t'^{5/2}(t'-t)}\right]. \tag{4}$$

The effect of the other cut, starting at $t=t_a$, is approximated as a series in Laguerre polynomials with exponential weight function in terms of a parabolic conformal mapping variable Z (Refs. 1, 2, and 4),

$$N(t)=e^{-\alpha Z}\sum_m g_m L_m(2\alpha Z) \tag{5}$$

with

$$Z(t)=\left\{\ln\left[\left[\frac{-t}{t_a}\right]^{1/2}+\left[-\frac{t}{t_a}+1\right]^{1/2}\right]\right\}^2. \tag{6}$$

Note that the a_i's and α occurring in Eqs. (2) and (5), respectively, are unknown parameters to be determined from data fitting.

In the case of the deuteron, the value of t_a was taken to be the anomalous cut position. For the ^{4}He form factor, the next nearest normal cut position starts at $t=25m_\pi^2$. But there are several anomalous cuts that are nearer to the origin of the t plane than the five-pion cut as can be found from computations carried out in the next section. We find that a better description of the data results if we take t_a to correspond to a suitable anomalous-cut position instead of the five-pion cut. For the first M significant terms, the series (5) can be rewritten as

$$N(t)=e^{-\alpha Z}\sum_{m=0}^{M} e_m Z^m. \tag{7}$$

With the approximations given by Eqs. (2) and (7), the form factor represented by Eq. (1) satisfies a general type of asymptotic behavior:

$$|F(t)|\to\frac{(\ln t)^{2m}}{t^n}\exp[-\alpha(\ln t)^2] \tag{8}$$

with $m,n=0,1,2,\ldots$. A simple dimensional quark-counting rule (DQCR) predicts $\alpha=m=0$ and $n=11$ for the ^{4}He charge form factor, but scaling violations in the inelastic structure functions would modify this type of asymptotic behavior by powers of $\ln t$. Modification of power falloff of form factors at $t\to\infty$ by exponential functions might arise in the type of models discussed in Ref. 2.

It may be possible that the zeros of the N function may exist in the physical region of the t plane, thus accounting for the observed dip in the form-factor data. Also the zeros of the $D(t)$ function might yield resonances on extrapolation, if they are nearer to the real axis in the time-like region. On the other hand, if the zeros of $D(t)$ are complex and their imaginary parts are large, the resonances would not be observed.

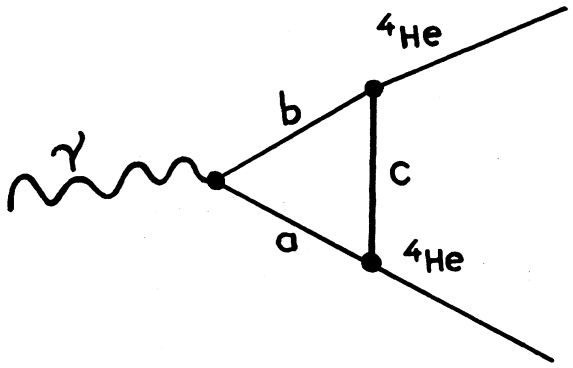

FIG. 1. Vertex graph for computation of the anomalous cuts of the ^{4}He form factor as described in the text.

III. COMPUTATION OF THE ANOMALOUS-CUT POSITIONS

The method of computation of anomalous-cut positions[5] using different vertex graphs has been discussed extensively in the literature,[5] using Landu-Bjorken rules[5] for the vertex shown in Fig. 1. The condition of an anomalous threshold can be written as

$$\begin{vmatrix} 1 & Y_{bc} & Y_{ca} \\ Y_{bc} & 1 & Y_{ab} \\ Y_{ca} & Y_{ab} & 1 \end{vmatrix}=0, \tag{9}$$

where

$$Y_{ab}=\frac{m_a^2+m_b^2-t}{2m_a m_b}, \tag{10}$$

$$Y_{bc}=\frac{m_b^2+m_c^2-M^2}{2m_b m_c}, \tag{11}$$

$$Y_{ca}=\frac{m_c^2+m_a^2-M^2}{2m_c m_a}. \tag{12}$$

In Eqs. (10–(12), m_a, m_b, and m_c stand for masses of the objects a, b, and c, respectively, in Fig. 1 and M stands for the mass of the ^{4}He nucleus. Solving the determinant Eq. (9) with definitions (10), (11), and (12) yields the following expression for the cut position in the t plane:

$$-t=\left[\frac{1}{2m_c^2}\{(m_b^2+m_c^2-M^2)(m_c^2+m_a^2-M^2)\right.$$
$$\pm[16m_a^2m_b^2m_c^4+(m_b^2+m_c^2-M^2)^2(m_c^2+m_a^2-M^2)^2-4m_b^2m_c^2(m_c^2+m_a^2-M^2)^2$$
$$\left.-4m_c^2m_a^2(m_b^2+m_c^2-M^2)^2]^{1/2}\}\right]-(m_a^2+m_b^2). \tag{13}$$

Using formula (13) and various possible exchanges of particles, nuclei, or their combinations for each of the objects a, b, and c, we have calculated the anomalous-cut positions. As in the case of the deuteron it is natural to suppose that simple and familiar exchanges corresponding to $^4\text{He}\to d+d$, $^4\text{He}\to{}^3\text{He}+n$, and $^4\text{He}\to{}^3\text{H}+p$ transitions might lead to anomalous-cut positions below the three-pion cut. But our computations using formula (13) shows that this is not really true. For all cases with $a=b$, the minus root gives $t=0$, whereas the plus root yields

$$-t=\Delta(m_a{}^2,m_c{}^2,M^2)/M_c{}^2 \tag{14}$$

with

$$\Delta(m_a{}^2,m_c{}^2,M^2)=m_a{}^4+m_c{}^4+M^4-2m_a{}^2m_c{}^2 -2m_a{}^2M^2-2m_c{}^2M^2 . \tag{15}$$

Applying this to the $^4\text{He}\to d+d$ case we obtain

$$-t=\frac{M^2}{M_d{}^2}(M^2-4M_d{}^2)\simeq 32M_N(2B_d-B_{\text{He}}) ,$$

where M_N is the nucleon mass and B_d and B_{He} denote binding energies of the deuteron and ^{4}He, respectively. Using the standard values $M_N=938.5$ MeV, $B_d=2.225$ MeV, and $B_{\text{HE}}=28.3$ MeV gives $t_a=0.717$ GeV^2, which lies farther away than the five-pion cut. Similar calculations for $^4\text{He}\to{}^3\text{He}+n$ and $^4\text{He}\to{}^3\text{H}+p$ yields the anomalous-cut positions at $t_a=0.205$ and 0.190 GeV^2, respectively. Results of our calculations using vertex graphs with these and more complicated intermediate states are summarized in Table I, where t_a ($t_{\min}$) stands for the t value obtained from Eq. (13) using the plus (minus) root. Since the right-hand side of Eq. (13) is symmetric in $m_a\leftrightarrow m_b$, we note that the (b,a,c) combination at the vertex of Fig. 1 yields the same value of the anomalous cut as (a,b,c). Table I is by no means exhaustive as it may be possible to imagine more complicated intermediate states than those considered here; but we have verified that they yield cut positions farther away than the five-pion cut.

TABLE I. Computation of anomalous-cut positions with various exchanges, a, b, and c in the vertex graph of Fig. 1.

			Anomalous-cut position	
a	b	c	t_a (GeV^2)	$t_{\min}$ (GeV^2)
n	n	^{3}He	0.205	0
d	d	d	0.717	0
p	p	^{3}H	0.190	0
p	$N^*(1470)$	$^3\text{H}\pi^0$	2.708	0.247
n	$N^*(1470)$	$^3\text{He}\pi^0$	2.720	0.245
n	$p\pi^-$	^{3}He	0.759	0.182
n	$n\pi^0$	^{3}He	0.747	0.173
d	$d\pi^0$	$d\pi^0$	5.864	0.163
$d\pi^0$	$d\pi^0$	d	4.909	0
$p\pi^0$	$N^*(1470)$	^{3}He	2.502	0.102
n	$n\pi^0$	$^3\text{He}\pi^0$	1.970	0.064
p	$p\pi^0$	$^3\text{H}\pi^0$	1.956	0.063
$p\pi^-$	$N^*(1470)$	$^3\text{He}\pi^0$	3.552	0.066
$n\pi^0$	$n\pi^0$	$^3\text{He}\pi^0$	2.701	0
$d\pi^0$	$d\pi^0$	$d\pi^0$	7.827	0
$p\pi^-$	$p\pi^-$	^{3}He	1.670	0

Although formula (13) gives two roots in general, only one of them yields the correct anomalous-cut position. For cases with $a=b$, the minus root corresponding to $t_{\min}$ yields incorrect cut position while t_a gives the correct one. In all simple and complicated cases considered in Table I $t_a>9m_\pi{}^2$. Only in cases of complicated (a,b,c) combinations like $(p\pi^0,N^*,{}^3\text{He})$, $(n,n\pi^0,{}^3\text{He}\pi^0)$, and $(p\pi^-,N^*,{}^3\text{He}\pi^0)$ for which $a\neq b$, the minus root yields $t_{\min}<9m_\pi{}^2$. But from the analogy of the simple cases with $a=b$ it is likely that only the t_a values yield the right cut positions also in the cases with $a\neq b$.

IV. ANALYSIS OF THE FORM-FACTOR DATA

Using the modified N/D method as described in Sec. II, we report in this section the results of our data analysis on the ^{4}He charge form factor.

We have collected 112 data points reported by various experimental groups with appropriate errors.[6–9] The normalization errors for the data of Refs. 6 and 7 have been quoted as 2% and 6%, respectively.[6] We have also taken the normalization error of the older data of Ref. 8 to be 6%. For the sake of convenience in data fitting we use the N function in the form (7) along with the formula (6) for Z. Using the normalization condition $e_0=a_0$ and taking $t_a=25m_\pi{}^2$ we first searched for the values of the parameters in formulas (1), (2), and (7) to obtain the best fit. Setting $\alpha=0$, which corresponds to the absence of the exponential weight function, yielded a very large value of total χ^2, but the χ^2 value reduced drastically when the exponential weight function was included ($\alpha\neq 0$). It may be noted that this exponential weight function has been also found to be essential for the deuteron form factors,[2] although for hadrons, good fits have been obtained in its absence. A fit to the available data with $t_a=25m_\pi{}^2$ has been obtained by retaining three terms in each series, (2) and (7) as shown by the dot-dashed curve in Fig. 2, and yields a total χ^2 value as 179 and $\chi^2/\text{DF}=1.68$. The six unknown parameters of this fit are given in Table II. As can be seen from Fig. 2, this fit yields a reasonably good description of the available data except around the secondary-maximum region where it deviates significantly from data points. Increasing the number of parameters in the N and the D functions did not improve the fit.

As noted in Sec. III there are a number of anomalous cuts which are nearer to $t=0$ than the five-pion cut. Therefore, as in the case of the deuteron,[2] it is reasonable to suppose that the contributions of some of them might be very significant in representing the form factor. In the next step of our analysis we tried to obtain good fits to the data choosing t_a as the anomalous-cut positions of Table I while assuming the D function as arising out of the three-pion cut in every case. This analysis was repeated for all values of the anomalous cuts of Table I existing below the five-pion cut, at first, with a total number of five-parameters and without including the Z^2 and highest-order terms in the $N(t)$ function, corresponding to the absence of a second dip and a third maximum. The best three of all such fits are shown by curves I, II, and III

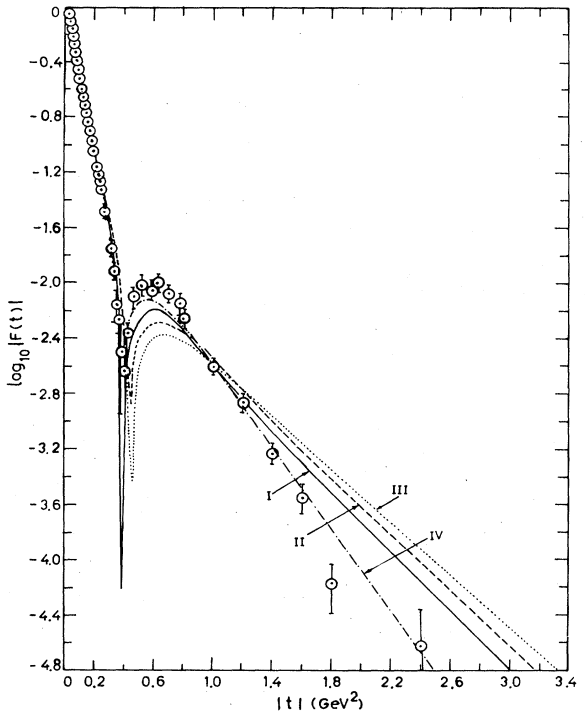

FIG. 2. Fits to the ^{4}He form-factor data as a function of various cut positions. Curves I, II, and III represent fits with $t_a=0.2478$, 0.205, and 0.190 GeV^2 and the first two terms in the N function but curve IV represents the fit with the five-pion cut at $t_a=25m_\pi{}^2$ and the first three terms in the N function.

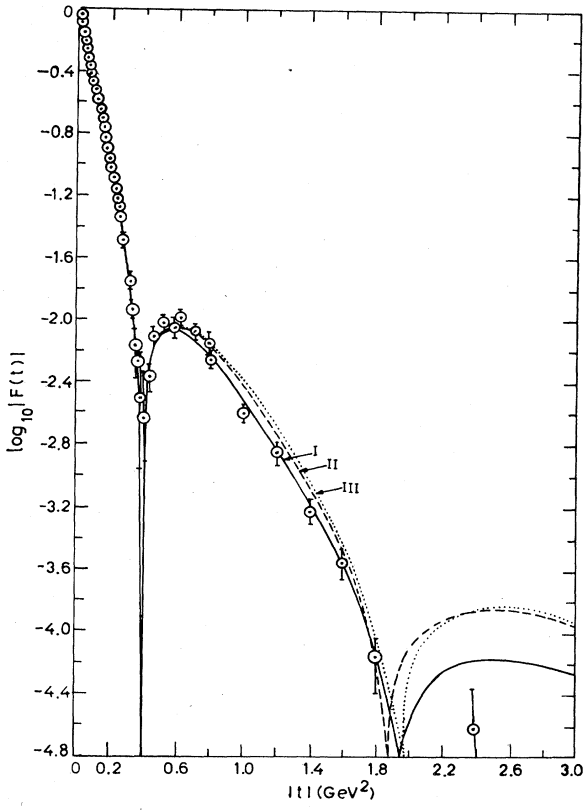

FIG. 3. Fits to the ^{4}He form-factor data with different anomalous-cut positions. Curves I, II, and III represent fits with three terms in the N function for $t_a=0.2478$, 0.205, and 0.190 GeV^2, respectively.

of Fig. 2 which correspond to anomalous-cut positions $t_a=0.247$, 0.205, and 0.190 GeV^2, respectively. When the Z^2 term was added to the $N(t)$ function, the fits improved significantly. These fits are shown in Fig. 3 by curves I, II, and III with $\chi^2/\mathrm{DF}=1.43$, 2.26, and 2.64, respectively. Thus, the best of all the fits were obtained by taking the contributions of the three-pion cut in the D function and the anomalous cut at $t_a=0.247$ GeV^2 in the N function. Although, visually, the fits appear to be reasonably good for the anomalous-cut positions, $t_a=0.205$ or 0.190 GeV^2, the total χ^2 value in these cases is significantly larger than the case with $t_a=0.247$ GeV^2. To discriminate more clearly between the fits with $t_a=0.247$ GeV^2 and $t_a\simeq 0.205$ GeV^2 more data points in the region, $1\leq|t|\leq 3$ GeV^2, are needed. The parameters for fits I, II, and III of Fig. 3 and fit IV of Fig. 2 are reported in Table II.

TABLE II. Unknown parameters of the analytic representation obtained from data analysis for the four fits where fits I, II, and III correspond to curves I, II, and III of Fig. 3 with the anomalous-cut positions at $t_a=0.2478$, 0.205, and 0.190 GeV^2, respectively, but fit IV corresponds to curve IV of Fig. 2 with the five-pion cut in the t plane. Here g_i's are the coefficients of the optimized polynomial expansion of the N function.

	I	II	III	IV
t_a (GeV^2)	0.2478	0.205	0.190	0.49
χ^2/DF	1.43	2.26	2.64	1.68
α	1.7591	1.4768	1.3966	3.779
a_0 (GeV^2)	1.8342	2.3582	0.1396	0.97
a_1	0.2477	0.2346	0.2325	0.1636
a_2 (GeV^{-2})	2.4536	2.4305	2.4389	0.2506
e_0 (GeV^2)	1.8342	2.3582	2.3488	0.97
e_1 (GeV^2)	−2.2559	−2.5147	−2.3803	−1.848
e_2 (GeV^2)	0.54	0.54	0.4888	0.548
g_0 (GeV^2)	1.2802	1.6305	1.6219	0.744
g_1 (GeV^2)	0.4667	0.6038	0.6015	0.206
g_2 (GeV^2)	0.0872	0.1237	0.1253	0.019

V. SOME RELEVANT INFORMATION

In this section we report useful information relating to the ^{4}He nucleus and its charge form factor that can be obtained from the results of data analysis described in Sec. IV.

A. Information relating to analyticity, convergence, and zeros of the form factor

It is clear from curve IV of Fig. 2 that the five-pion cut in the N function along with the three-pion cut in the D function can describe the data in the available spacelike

region reasonably well, although there are significant deviations around the second maximum. The best fit is obtained as in the case of curve I of Fig. 3 if the five-pion cut is replaced by the anomalous cut at $t_a=0.2478$ GeV^2. However the anomalous cuts arising out of $(p,p,^3\text{H})$ and $(n,n,^3\text{He})$ exchanges appear visually to yield nearly the same fits, but with larger χ^2/DF values. Other anomalous cuts yield fits worse than these and are therefore, much less important. As noted earlier, the presence of the exponential weight function which occurs naturally in Laguerre polynomial expansion is essential in both cases for improving the fits. Also the convergence of the OPE (5) proposed for the N function appears to be good in both cases. To verify this we calculated the coefficients, g_i, using the computed values of e_i, as shown in Table II for four different fits. It is clear that the successive coefficients in OPE decreases at a good rate. Besides, in the series occurring in the D function, no higher-order coefficients beyond a_2 seem to be important. As envisaged in Secs. I and II, all the fits yield the correct dip structure in the existing experimental data corresponding to a zero of the N function at $|t|\simeq 0.39$ GeV^2, but each fit requires a second zero and correspondingly a third maximum existing in the physical region accessible to the available range of experiments. The positions of the second zero (third maximum) is predicted at $|t|=1.94$ (2.44), 1.87 (2.5), and 1.89 (2.54) GeV^2 for curves I, II, and III, respectively, of Fig. 3, and at $|t|=3.0$ (3.4) GeV^2 for curve IV of Fig. 2. In the future, the presence of the second zero and the third maximum could be verified by more accurate experimental data on $e\,^4$He scattering in the range $1.8\leq|t|\leq 4.0$ GeV^2 and might discriminate the importance of the five-pion cut as against the three anomalous cuts. The positions of zeros and different maxima are summarized in Table III along with other physical quantities for all the four fits.

TABLE III. Different physical quantities obtained from the present data analysis.

Physical quantities	I	II	III	IV
Root-mean-square radius (fm)	1.66	1.70	1.71	1.80
Half-density radius (fm)	1.337	1.37	1.38	1.4
Position of first zero (GeV^2)	0.39	0.39	0.39	0.39
Position of second zero (GeV^2)	1.94	1.87	1.89	3.0
Position of second maximum (GeV^2)	0.58	0.58	0.58	0.58
Position of third maximum (GeV^2)	2.44	2.5	2.54	3.4

B. Extrapolation of the form factor and its asymptotic behavior

Using the results of Table II and formulas (2) and (7), we find that the experimental data favor the asymptotic behavior

$$F(t)\underset{t\to\infty}{\longrightarrow}\exp[-\alpha(\ln t)^2](\ln t)^4/t^2\,, \tag{16}$$

where $\alpha=1.7591$, 1.4768, and 1.3968 for curves I, II, and III of Fig. 3, but $\alpha=3.779$ for curve IV of Fig. 2. It may be pointed out that this result is based upon extrapolation of the proposed fits onto $t\to\infty$ and therefore, may not be very reliable.[10] The extrapolated values of the form factor onto the timelike region in the case of fits I, II, and III corresponding to Fig. 3 with $t_a=0.2478$, 0.202, and 0.189 GeV^2, respectively, have been shown in Fig. 4 for smaller $|t|$ values. The extrapolation of fits I and II with $t_a=0.2478$ and 0.202 GeV^2, respectively, have been shown in Fig. 5 for larger $|t|$ values. It is clear from Fig. 4 that the extrapolation is smooth and shows a threshold enhancement at the effective cut position. Also the extrapolated curve does not show any evidence of resonance peaks as in the case of deuteron. The extrapolated curves for the other fits can be similarly plotted using the parameters of Table II. While obtaining these results it is necessary to mention that the form factor at larger $|t|$ values is likely to be less reliable because of the well-known fact that the error in the extrapolated quantity becomes larger as one moves farther away from the data region.[10]

C. Nuclear charge density and charge radius

With the best fit I we have computed the charge density $\rho(r)$ of the ^{4}He nucleus as a function of the nuclear radius using the well-known formula

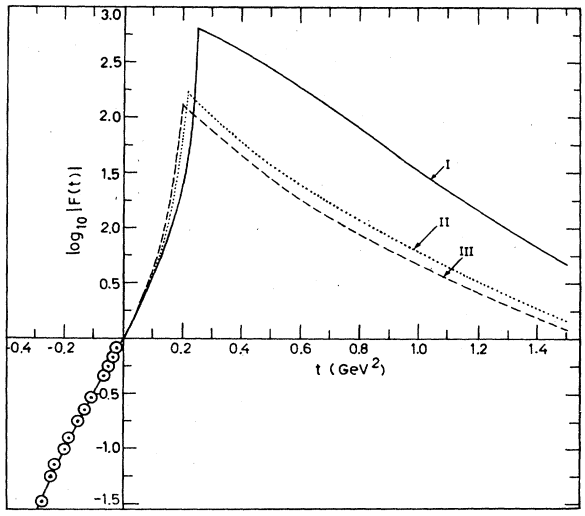

FIG. 4. Extrapolation of the ^{4}He form factor into the timelike region. Curves I, II, and III represent extrapolated values corresponding to the best fits of Fig. 3 with $t_a=0.2478$, 0.205, and 0.190 GeV^2, respectively.

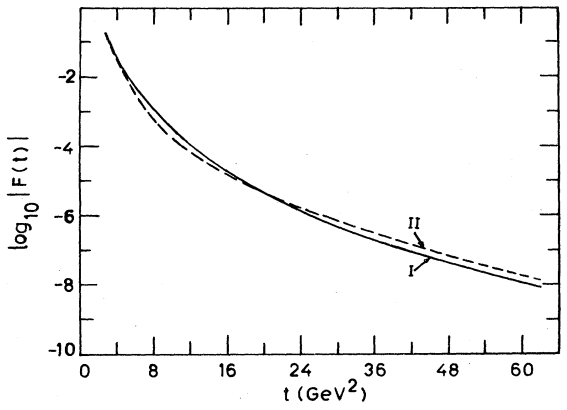

FIG. 5. Extrapolation of the ^4H_e form factor into large-t values of the timelike region. Curves I and II represent the extrapolated values corresponding to the best fits of Fig. 3 with $t_a=0.2478$ and 0.205 GeV^2, respectively.

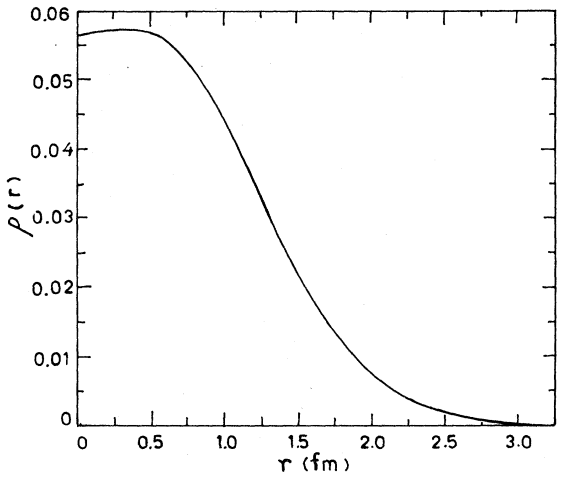

FIG. 6. Computation of charge density $\rho(r)$ as a function of nuclear radius r.

$$\rho(r)=\frac{1}{4\pi^2 r}\int_0^\infty F(|t|)\sin(r\sqrt{|t|})d|t| \ . \tag{17}$$

The computed values of $\rho(r)$ have been plotted against r in Fig. 6 showing a central depression. The charge density has a maximum at $r=0.34$ fm. The half-density radius obtained from such a computation is found to be 1.337 fm. It may be pointed out that the value of $\rho(r)$ near the center of the nucleus ($r=0$) is also uncertain to a certain extent as it is related to the asymptotic behavior of the form factor. The charge density for the other fits which can be plotted in a similar fashion also shows a central depression and a half-density radius nearly 1.4 fm as summarized in Table III. The most reliable of all results obtained by the present method is the root-mean-square charge radius

$$r_c=[6F'(0)]^{1/2} \tag{18}$$

which needs extrapolation of the form factor only up to $t=0$, and is computed to be 1.66, 1.7, 1.71, and 1.8 fm for fits I, II, III, and IV, respectively. Thus the five-pion cut yields a charge radius nearly 10—12% larger than the anomalous cuts.

VI. CONCLUSION

The present and earlier analyses suggest that the method of analytic representation of form factors which has been found successful for hadrons can also be used to parametrize the data on light nuclei like deuteron and ^{4}He, but with appropriate modifications. In the case of the deuteron, the nearest anomalous cut existing below the three-pion cut originates from the familiar simple vertex graph with p and n exchanges corresponding to the transition $d\to p+n$. In the case of ^{4}He all familiar and simple exchanges corresponding to $^4\text{He}\to d+d$, $^3\text{He}+n$, and $^3\text{H}+p$ are found to yield anomalous-cut positions above the three-pion threshold. Present analysis shows that the anomalous cuts existing between the three- and the five-pion thresholds play an important role in representing the form factor. The method also succeeds in obtaining useful information on charge density, charge radii, asymptotic behavior, and extrapolated values of form factors for light nuclei subject to the well-known limitations.[10] In the proposed N/D method the presence of the exponential weight function for the Laguerre polynomial expansion of the N function was not necessary for hadrons,[1] but seems to be very much necessary for deuteron[2] and ^{4}He as evident from this analysis. The best fit obtained by this analysis seems to favor strongly the presence of a second dip and a third maximum which can also be verified by future experimental measurements. To confirm such conclusions we plan to carry out such investigations for the charge and magnetic form factors of ^{3}He in a separate paper.

ACKNOWLEDGMENTS

One of us (M.K.P.) thanks the University Grants Commission, India for a research project and the other (K.N.A.) thanks the Commission and the management of Kendrapara College for the Teachers Fellowship.

[1]B. B. Deo and M. K. Parida, Phys. Rev. D **8**, 2939 (1973); **9**, 2068 (1974).

[2]M. K. Parida, Phys. Rev. D **19**, 3320 (1979); M. K. Parida, S. Patel, and K. N. Agrawalla, *ibid.* **27**, 1187 (1983).

[3]R. E. Cutkosky and B. B. Deo, Phys. Rev. **174**, 1859 (1968); S. Ciulli, Nuovo Cimento **61A**, 787 (1969).

[4]B. B. Deo and M. K. Parida, Phys. Rev. Lett. **26**, 1609 (1971).

[5]R. J. Eden, P. V. Landshoff, D. I. Olive, and J. C. Polk-

inghorne, *The Analytic S-Matrix* (Cambridge University Press, Cambridge, 1966); J. Hamilton, lectures given at the Neils Bohr Institute and NORDITA, Copenhagen, 1968 (unpublished).

[6]J. S. McCarthy, I. Sick, and R. R. Whitney, Phys. Rev. C **15**, 1396 (1977).

[7]R. F. Frosch, J. S. McCarthy, R. E. Rand, and M. R. Yearian, Phys. Rev. **160**, 874 (1967).

[8]R. W. McAllister and R. Hofstadter, Phys. Rev. **102**, 851 (1956).

[9]R. G. Arnold *et al.*, Phys. Rev. Lett. **40**, 1429 (1978).

[10]R. E. Cutkosky, Ann. Phys. (N.Y.) **54**, 110 (1969); S. Ciulli, G. Pomponiu, and I. Sabba Stefanescu, Phys. Rep. **17C**, 133 (1975). It has been pointed out in Ref. 3 and by these authors that the errors in extrapolated quantities arise due to the convergence and the stability problems, but they can be reduced using analyticity and optimized polynomial expansion. In the present paper, however, only the N function has been approximated by OPE, but the D function by an effective range formula obtainable using dispersion relation.